Biophysics and medical physics

Original article
DOI: https://doi.org/10.18721/JPM16209

DETERMINATION OF CONDITIONS FOR OBTAINING RADIOACTIVITY OF NITROGEN-13 ISOTOPE FOR MEDICAL USE BY NX2 DENSE PLASMA FOCUS DEVICE

A. Nassif [1] ✉, W. Sahyouni [2], O. Zeidan [2], N. Kafa [2]

[1] Al-Wataniya Private University, Hama, Syrian Arab Republic;

[2] Al-Baath University, Homs, Syrian Arab Republic

✉ alaa.nassif.85@hotmail.com

Abstract. In the paper, a theoretical study to calculate the value of the radioactivity of nitrogen-13 isotope required for use in positron emission tomography (PET) has been presented. The isotope is produced by deuteron beams from NX2 dense plasma focus device. First the effect of three factors was studied, namely, the deuterium gas density, exposure time and the repetition rate of the device. The results showed an increase in radioactivity as deuterium gas pressure decreased. It was next possible to obtain four radioactivity values, suitable for use in PET, by varying the two rest factors.

Keywords: nitrogen-13 isotope, NX2 dense plasma focus device, radioactivity

For citation: Nassif A., Sahyouni W., Zeidan O., Kafa N., Determination of conditions for obtaining radioactivity of nitrogen-13 isotope for medical use by NX2 dense plasma focus device, St. Petersburg State Polytechnical University Journal. Physics and Mathematics. 16 (2) (2023) 98–110. DOI: https://doi.org/10.18721/JPM.16209

Научная статья
УДК 533.9.07
DOI: https://doi.org/10.18721/JPM.16209

ОПРЕДЕЛЕНИЕ УСЛОВИЙ ПОЛУЧЕНИЯ РАДИОАКТИВНОСТИ ИЗОТОПА АЗОТ-13, ТРЕБУЕМОЙ ДЛЯ МЕДИЦИНСКОГО ПРИМЕНЕНИЯ ПРИ ИСПОЛЬЗОВАНИИ УСТРОЙСТВА ПЛАЗМЕННОЙ ФОКУСИРОВКИ NX2

А. Нассиф [1] ✉, В. Сахьюни [2], О. Зейдан [2], Н. Кафа [2]

[1] Частный университет Аль-Ватания, г. Хама, Сирийская Арабская Республика;

[2] Университет Аль-Баас, г. Хомс, Сирийская Арабская Республика

✉ alaa.nassif.85@hotmail.com

Аннотация. В работе представлено теоретическое исследование, направленное на расчет значений радиоактивности изотопа ^{13}N, необходимых для медицинского применения в позитронно-эмиссионной томографии (ПЭТ). Изотоп можно получать путем ядерной реакции ^{12}C(d, n)^{13}N, реализуемой пучками дейтронов из устройства фокусировки плотной плазмы NX2. На первой стадии исследования изучалось влияние на уровень радиоактивности трех параметров устройства NX2: давления газообразного дейтерия (ДГД), времени экспозиции и частоты следования импульсов. Результаты показали рост уровня радиоактивности по мере снижения ДГД. На второй стадии удалось получить четыре значения радиоактивности, пригодные для использования в ПЭТ, путем подбора значений двух других факторов.

Ключевые слова: изотоп азот-13, радиоактивность, устройство плазменной фокусировки NX2, пучок дейтронов

Для цитирования: Нассиф А., Сахьюни В., Зейдан О., Кафа Н. Определение условий получения радиоактивности изотопа азот-13, требуемой для медицинского применения при использовании устройства плазменной фокусировки NX2 // Научно-технические ведомости СПбГПУ. Физико-математические науки. 2023. Т. 16. № 2. С. 98–110. DOI: https://doi.org/10.18721/ JPM.16209

Introduction

Since the initial design of the dense plasma focus devices by J. W. Mather [1] and N. V. Filippov et al. [2], a large number of studies have been conducted on this phenomenon due to its distinction in terms of obtaining very hot, very dense plasma that constitutes a source for a large number of radioactive emissions and ion beams and electrons, depending on the type of gas used in the operation process [3].

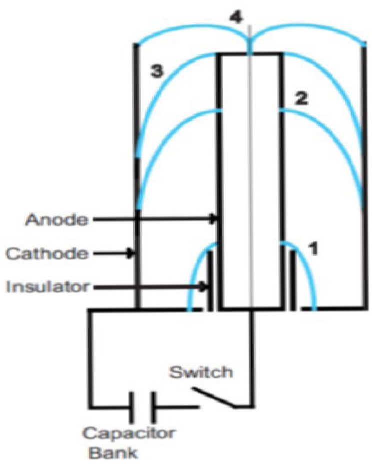

Fig. 1. Scheme of the dense plasma focus device able to cause the nuclear reaction required for the production of short-lived radioactive isotopes, e. g. ^{13}N

In Fig. 1 one can see an elementary scheme of this device. In the process of evolving plasma, a focus known as "pinch" is formed; it is a small column of plasma that collapses after a very short period (ns) due to the instability of the plasma [4, 5], leading to beams of ions and electrons moving in opposite directions [6]. The properties of these beams have been studied and characterized with a view to their practical application such as thin film deposition [7 – 11], material synthesis [12 – 15] and the production of short-lived radioisotopes [16, 17].

In the case when deuterium gas is used in a dense plasma device, it is possible to take advantage of the energy ion beams produced after the collapse of the plasma pinch and its collision with a suitable target in order to cause the desired reaction. For this purpose, many researches have been conducted experimental and computational studies aimed at the possibility of benefiting from the ion beams emitted by the collapse of a plasma column formed in the dense plasma focus device, especially when using deuterium as working gas in order to bring about the nuclear reaction required for the production of short-lived radioactive isotopes. M. Sumini et al. [18] designed a 150 kJ dense plasma focus device operating in a 1 Hz frequency mode to produce the ^{18}F radioactive isotope (1 Ci in a time of 2 hrs) and put the engineering designs of the electrodes and the parameters of the electrical circuit, and 128 shots were carried out. B. Shirani et al. [19] also studied the possibility of obtaining the radioactive isotope ^{13}N from a low-energy dense plasma focus device, and a radioactivity value of 10 kBq for one shot was obtained. In the process, the radioactivity value increased to several tens of MBq at an operating rate of f = 1 Hz with an operating time of 600 s. Since the medically required radioactivity is about 4 GBq, the idea to change the design of the electrodes or the pressure of deuterium gas was put forward. In order to increase the energy of the outgoing deuterons spectrum, M. Akel et al. [20] conducted numerical experiments using the Lee code for calculating the characteristics of the ion beams emitted by a number of dense plasma devices with different operating energies and for calculating the radioactivity of the $^{12}C(d, n)^{13}N$ reaction. As a result, they found that the device should operate in a repetitive mode (the repetition rate was f = 25 Hz for an operation period of 600 s) to reach the value of the medically required radioactivity and came to the conclusion that this possibility of operation was not available in the current devices. In addition, there was a problem of endurance of targets to resulting thermal loads.

In 2019, H. Sadeghi et al. [21] developed the idea of adding magnetic lenses in order to focus and direct the outgoing ion beams, as well as to reduce the scattering ratio. Simulations were carried out on 16 different plasma incinerators with different energies (from 400 J to 500 kJ) and a radioactivity value of 0.016–7.71 GBq was reached. It was established that 9 of the devices studied were able to achieve the medically required radioactivity value of the isotope ^{13}N by using this technique.

Research technique

Firstly, the number of deuterium ions emitting from the collapse of the plasma pinch was found, then the radioactivity of the isotope was calculated for the 3 Torr pressure deuterium gas. Secondly, the effect of changing the pressure of deuterium gas on the value of radioactivity was calculated. Thirdly, the advantage of repetitive operation of the studied plasma focus device NX2 was taken in order to explore the effect of the exposure time and repetition rate on radioactivity. The results obtained are presented next.

Results and discussion

Finding deuterons beam properties emitted by a NX2 dense plasma focus device. The number of generated ions was calculated by taking advantage of the parameters of the plasma pinch (the source) that were found using the Lee code, by taking advantage of the following device features [22]:

Operating potential V = 14 kV;

Capacitor bank capacity C_0 = 28 μF;

Inductance L_0 = 20 nH.

The value of the total discharge current produced by the capacitor bank can be calculated as follows:

$$I_0 = \frac{V_0}{\sqrt{\frac{L_0}{C_0}}} = \frac{4\cdot 10^3}{\sqrt{\frac{20\cdot 10^{-9}}{28\cdot 10^{-6}}}} = 523.83\ \text{kA}. \tag{1}$$

The capacitor bank discharge time is

$$t_0 = \sqrt{L_0 C_0} = \sqrt{20\cdot 10^{-9}\cdot 28\cdot 10^{-6}} = 74.8\ \mu\text{s}; \tag{2}$$

$$T = 2\pi t_0 = 2\pi\cdot 74.8\cdot 10^{-6} = 469.98\ \mu\text{s}. \tag{3}$$

The time of movement of the plasma sheath through the axial phase is given by Ref. [23]:

$$t_a = \sqrt{\left[\frac{2\pi^2\left(c^2-1\right)}{\mu_0 \ln c}\right]}\left[\frac{\sqrt{f_m \cdot Z_0\sqrt{\rho}}}{f_c\left(\frac{I_0}{a}\right)}\right], \tag{4}$$

where c is the ratio of the cathode radius b to the anode one a ($c = b/a$ = 4.1/1.9 = 2.2); μ_0 is the permeability of the plasma, $\mu_0 = 4\pi\cdot 10^{-7}\ H/(m\cdot Z_0)$; Z_0 is the anode length; f_m, f_c are the factors of mass and current losses in the axial phase, relatively, f_m = 0.06, f_c = 0.70 [22].

The time of movement of the plasma sheath radially at the top of anode until reaching the stage of pinching is given by Ref. [23]:

$$t_r = \sqrt{\frac{4\pi}{\mu_0\left(\gamma+1\right)}}\left[\frac{\sqrt{f_m\sqrt{\rho}}}{f_c\left(\frac{I_0}{a}\right)}\right]a, \tag{5}$$

where γ is the specific heat capacity of deuterium plasma, $\gamma = 5/3$.

The density ρ (kg/m^3) of deuterium gas is calculated by the formula

$$\rho = P \cdot M / (R \cdot T). \tag{6}$$

Our studies showed that about 60 % of the total discharge current will form the peak current I_{peak} which continues to push the plasma sheath until reaching the stage of the formation of the plasma pinch [24]. Deuterium gas has $P = 3$ Torr where this condition is met by Lee code. Thus, we get that the pressure is

$$P = 3 \cdot 1.013 \cdot 10^5/760 = 400 \text{ Pa}.$$

The temperature $T = 273 + 20 = 293$ K; the gas constant $R = 8.31$ J/(K·mol); the molar mass of deuterium gas $M = 4.027$ kg/mol.

Substituting these values into Eq. (6) for the deuterium gas density, we obtain that

$$\rho = 0.661 \text{ kg/m}^3. \tag{7}$$

The values obtained were taken to calculate the velocity values of the plasma sheath in the axial and radial phases by using Lee code. The following are the results obtained:

The axial velocity $v_a = 1290$ km/s, (8)

The radial velocity $v_r = 327$ km/s, (9)

The ion current density is calculated using the Langmuir – Child formula [25]:

$$J_i = 1.86 \cdot \left(\frac{4}{9}\right) \varepsilon_0 \sqrt{\frac{2e}{m_i}} \cdot \frac{\Phi^{3/2}}{d^2}, \tag{10}$$

where ε_0 is the permittivity of free space, $\varepsilon_0 = 8.854 \cdot 10^{-12}$; e is the electric charge, $e = 1.6 \cdot 10^{-19}$ C; m_i is the mass of the deuterium ion, $m_i = 3{,}34 \cdot 10^{-27}$ kg; d is the width of the formed plasma sheath; Φ is the induced voltage within the plasma pinch,

$$\Phi = I_0\,(dL_p/dt). \tag{11}$$

We calculate the induction within the plasma pinch dL_p/dt by using Ref. [26]:

$$\frac{dL_p}{dt} = \frac{\mu_0}{2\pi}\left[\ln\left(\frac{b}{r_p}\right) v_a + \left(\frac{z}{r_p}\right) v_r\right], \tag{12}$$

where b, r_p are the radii of the cathode and plasma pinch, relatively, $b = 4.100$ cm, $r_p = 0.302$ cm; z is the length of the plasma pinch, $z = 2.806$ cm.

Substituting these values, we get that $dL_p/dt = 0.674$.

Thus, according to Eq. (11), the induced potential within plasma pinch is

$$\Phi = 523.83 \cdot 10^3 \cdot 0.674 = 353 \text{ kV}.$$

Now let us calculate ion current density:

$$J_i = 1.86 \cdot \left(\frac{4}{9}\right) \varepsilon_0 \sqrt{\frac{2e}{m_i}} \cdot \frac{\Phi^{3/2}}{d^2} = 19 \text{ kA/m}^2.$$

Thus we get the number of deuterium ions ejected from the plasma pinch:

$$N_i = \pi \frac{r_p^2}{e} J_i \tau_p = 6.5 \cdot 10^{12}\,(\text{ions}). \tag{13}$$

Calculation of the radiative yield. The energy distribution $f\,(E)$ of the ions emitted from the plasma pinch is given by Ref. [20]:

$$f\,(E) = dN_i / dE = C \cdot E^{-m}, \tag{14}$$

where C is the constant, power coefficient m takes values within the range $2.0 < m < 3.5$;

$$N_i = \int_{E_{min}}^{E_{max}} CE^{-m} dE = C\left[\frac{E^{1-m}}{1-m}\right]_{E_{min}}^{E_{max}}.$$

Consequently, the function $f(E)$ is of the form

$$f(E) = N_i\left(\frac{1-m}{E_{max}^{1-m} - E_{min}^{1-m}}\right)E^{-m}. \quad (15)$$

where E_{max}, E_{min} are the maximum and minimum energies of the emitting deuterons.

The radiative yield of the reaction is given by Ref. [27]:

$$\langle y\rangle = \frac{\Omega_1}{\Omega_2}\left(\frac{1-m}{E_{max}^{1-m} - E_{min}^{1-m}}\right)\int_{E_{min}}^{E_{max}} n\frac{E^{-m}\sigma(E)}{\frac{dE}{dx}}dE. \quad (16)$$

where Ω_1, Ω_2 are the solid angles of the source (the pinch) and of the target, relatively; n is the density of graphite target, $n = 1.129\cdot10^{29}$ m^{-3}; dE/dx is the stopping power of the graphite target; $\sigma(E)$ is the experimental cross-section of the reaction $^{12}C(d, n)^{13}N$.

There are two angles Ω_1 and Ω_2 that need to be calculated: the former is the angle of emission of ions from the pinch, and the latter is the angle of arrival of ions to the target.

Deuterium ions are emitted in the form of a cone whose top rests on the grip and its base does on the target. The solid angle of a cone is given by

$$\Omega_1 = 2\pi(1 - \cos\theta_1). \quad (17)$$

If we assume that the angle $\theta_1 = 25° = 0.436$ rad, then $\Omega_1 = 0.587$ sr.

The portion of the released ions falls on the graphite target. The angle of arrival of ions to the target is proportional to the surface area and is given by the following relationship:

$$\Omega_2 = \pi\theta_2 = \pi(r/R)^2, \quad (18)$$

where r is the radius of the source, R is the distance between the target and the source (the grip).

If we assume that $r = 1$ cm and $R = 20$ cm, then $\Omega_2 = 0.0078$ sr.

Calculation of the stopping power *dE/dx* of a graphite target. The 2013 SRIM (The Stopping and Range of Ions in Matter) program (see Ref. [28]) was used to find the stopping power of deuterium ions within the energy range 0.6 – 3 MeV within the graphite target. By drawing the matching curve, we obtained the formula for the stopping power: $dE/dx = 51408E^{-0.691}$.

The results obtained are shown in Table 1 and Fig. 2.

Table 1

The ion energy – the stopping power relationship obtained using SRIM

Ion kinetic energy, MeV	Stopping power, GeV/m
0.60	71.6
0.70	65.0
0.90	55.5
1.00	51.9
1.10	49.0
1.50	39.4
1.70	36.0
1.80	34.5
2.00	32.0
2.50	27.1
2.75	25.3
3.00	23.7

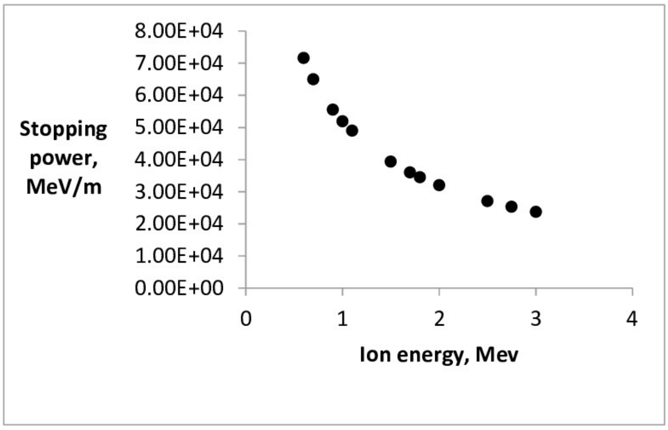

Fig. 2. The dependence of the stopping power of deuterium ions within the graphite target on their kinetic energy

Finding the experimental cross-section σ(*E*) for the reaction $^{12}C(d, n)^{13}N$. To find this cross-section, the Experimental Nuclear Reaction Data (EXFOR) of the International Atomic Energy Agency (IAEA) (see Ref. [29]) was used. This result is presented in Fig. 3 and Table 2. Thus, we obtained the formula giving the cross-section:

$$\sigma(E) = -72.771E^2 + 314E - 164.78.$$

Table 2

Experimental dependence of cross-section values on the ion energy for the $^{12}C(d, n)^{13}N$ reaction (taken from EXFOR database)

Ion kinetic energy *E*, Mev	σ, mb
0.65	12.37
1.04	82.29
1.52	130.2
2.00	186.5
3.00	119.9

Substituting the previous relations to calculate the yield value at the values m = 2.0, 3.0, 3.5, we can find three $\langle y \rangle$ values. They are equal respectively:

$$9.3100\cdot10^{-5},\ 1.4534\cdot10^{-5},\ 3.1420\cdot10^{-5}.$$

The radioactivity is calculated by Ref. [20]:

$$A = N_i \langle y \rangle \ln2/T_{1/2}, \qquad (19)$$

where $T_{1/2}$ is the half-life of the radioactive isotope ^{13}N, $T_{1/2}$ = 10 min = 600 s.

Therefore, the value of the radioactivity for $m = 2$ is: $A = 6.99\cdot10^5$ Bq.

The effect of the density of deuterium gas on the value of radioactivity. The density of deuterium gas is considered as one of the factors affecting the formation of the plasma sheath, its axial and radial velocity, and the parameters of the plasma pinch formed at the end of radial phase, and thus, its effect on the induction generated within the pinch and the voltage generated within it, and later on the current density and the number of ions emitting from the collapse of the pinch.

The calculations of the density of the gas when changing the pressure of deuterium gas from the value P = 1 Torr to the value at which focusing does not occur, and then finding the values of the velocities of the axial and radial plasma sheath, the dimensions and the duration of the formed plasma pinch using the Lee code were performed. The results obtained are presented in Table 3.

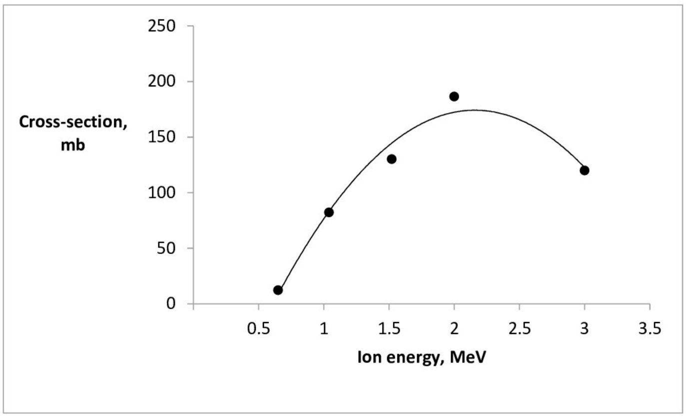

Fig. 3. Cross-section of the $^{12}C(d, n)^{13}N$ reaction (taken from (EXFOR) database)

Table 3

The dependence of some key plasma parameters on the deuterium gas pressure and density using the Lee code

Deuterium gas		Plasma sheath velocity		Plasma pinch		
Pressure, Torr	Density, g/m^3	Axial, km/s	Radial, km/s	Radius, mm	Length, mm	Duration, ns
1	220	176	457	3.01	28.06	13.5
2	440	145	371	3.02	28.04	16.7
3	661	129	327	3.04	28.06	19.1
4	881	118	297	3.05	28.04	21.0
5	1102	111	274	3.06	28.05	22.8
6	1322	105	257	3.08	28.03	24.3
7	1543	100	243	3.09	28.02	25.8
8	1763	95	231	3.11	28.05	27.3
9	1984	92	221	3.12	28.03	28.6
10	2204	89	211	3.13	28.03	30.0
11	2424	86	203	3.15	28.05	31.4
12	2645	83	195	3.17	28.02	32.6
13	2865	81	189	3.18	28.04	33.9
14	3086	79	183	3.20	28.03	35.2
15	3306	77	176	3.22	28.04	36.5
16	3527	75	171	3.24	28.05	37.7
17	3747	74	166	3.26	28.04	39.0
18	3968	72	161	3.28	28.04	40.3
19	41885	71	157	3.30	28.02	41.6

The value of the plasma pinch induction, the voltage generated within it, the density of the ion current and the number of the ejected ions were calculated using Eqs. (10) – (13) (see Table 4). Then, using Eq. (19), the value of the radioactivity was calculated with changing in the deuterium gas pressure. The results are shown in Fig. 4.

Table 4

The dependence of some plasma pinch and deuterium ion beam parameters on the deuterium gas pressure using the Lee code

Deuteriun gas pressure, Torr	Plasma pinch		Deuteriun ion beam	
	Induction	Voltage in it, kV	Current density, kA/m^2	Number of ejected ions
1	0.9439	494.5	31.64	660
2	0.7645	400.5	23.09	595
3	0.6707	351.4	18.95	559
4	0.6074	318.2	16.35	530
5	0.5599	293.3	14.46	509
6	0.5221	273.5	13.04	489
7	0.4924	257.9	11.95	475
8	0.4656	243.9	10.97	462
9	0.4444	232.8	10.24	452
10	0.4237	221.9	9.534	441
11	0.4056	212.5	8.919	432
12	0.3872	202.8	8.336	419
13	0.3747	196.3	7.924	414
14	0.3608	189.0	7.495	407
15	0.3457	181.1	7.022	395
16	0.3341	175.0	6.668	388
17	0.3230	169.2	6.342	382
18	0.3116	163.2	6.010	374
19	0.3023	158.4	5.753	369

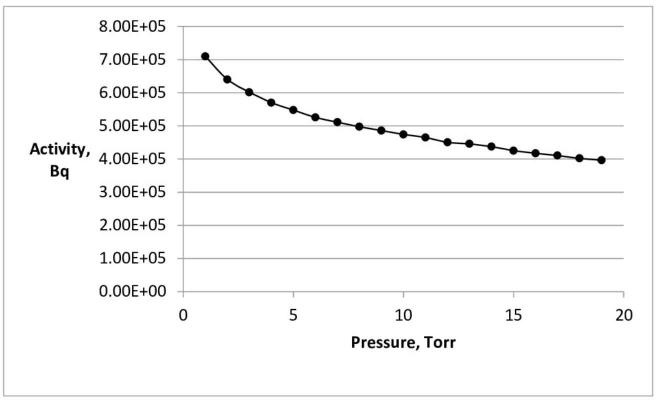

Fig. 4. The plots of the radioactivity values versus the deuterium gas pressure

An analysis of the obtained results allows us to note that an increase in the pressure of deuterium gas has led to an increase in the time of movement of the plasma sheath both axially and radially and consequently decreasing of axial velocity of the plasma from 176 km/s at a pressure of 1 Torr to 71 km/s at the highest pressure value (19 Torr), and the plasma velocity at the top of the anode radially decreased from 457 km/s to 157 km/s, and thus, the decrease in the value of the energy coming from the capacitor bank to the plasma pinch, and as a result the decrease in the value of the induction inside the plasma pinch and the voltage generated within it, and thus, the number of ions ejected from the plasma pinch according to Eqs. (11) – (13), the value of the radioactivity of the isotope ^{13}N decreases, as shown in Fig. 3, from 710 kBq to 397 kBq. So, decreasing the gas pressure led to an increase in the radioactivity value of the isotope ^{13}N, but in order to make it suitable for use in medicine, rather in PET, the radioactivity value must be within the range 370 – 740 MBq [30] and therefore it is necessary to search for additional methods for increasing the value of radioactivity, apart from the low pressure of deuterium gas, such as increasing the device's operating rate, i. e., exposure of the target to a number of successive shots (i. e., increasing reaction yield) or by increasing the operating power of the device.

Calculation of the radioactivity value when changing the frequency of operation and exposure time. The value of the radioactivity of the isotope ^{13}N was found at repetition rates equal to 1, 5, 10, 16 Hz and the exposure time of the graphite target to deuterium ions equal to 30, 60, 100, 200, 300, 400, 500 s.

The value of the radioactivity was calculated according to the formula given in Ref. [20]:

$$A_\nu = N_i \cdot \langle y \rangle \, \nu[1 - \exp(-\lambda t)], \quad (20)$$

where ν is the frequency of shots, $\lambda = (\ln 2)/T_{1/2}$ ($T_{1/2}$ is the radioactive half-period); t is the exposure time.

The calculation results are presented in Table 5 and Fig. 5.

Table 5

The dependence of the radioactivity values on the exposure time at different values of the repetition rate

Exposure time, s	Radioactivity value, MBq			
	1 Hz	5 Hz	10 Hz	16 Hz
30	18.9	94.3	189	302
60	34.9	174	349	**558**
100	53.8	269	**538**	861
200	97.8	**489**	978	1560
300	133.0	**666**	1330	2130
400	164.0	818	1640	2620
500	189.0	944	1890	3020

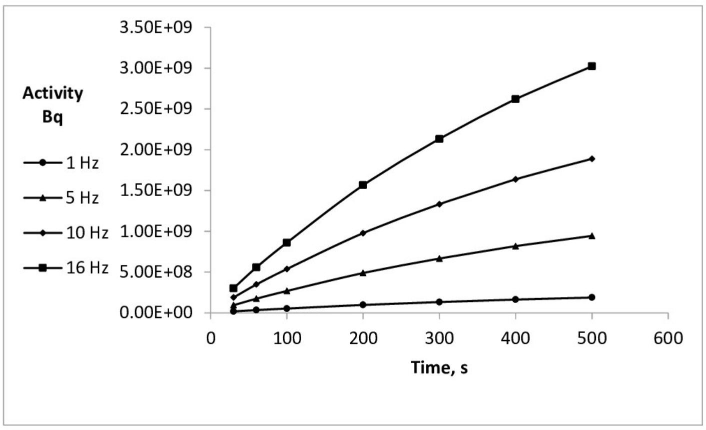

Fig. 5. Plots of the radioactivity values versus the exposure time at different repetition rates

Table 6

The radioactivity values that meet the requirements for use in PET

Radioactivity value, MBq	Exposure time, s	Repetition rate, Hz
489	200	5
538	100	10
558	60	16
666	300	5

It is evident from the results shown in the Table 5 and Fig. 5, that there are four values for the radioactivity of the isotope for use in a PET technique. We specially listed these values in ascending order in the separate Table 6.

Conclusions

This study presents a visualization of the operational conditions that should be met in the NX2 dense plasma focus device as a medium-energy apparatus for the possibility of producing ^{13}N isotope suitable for use in PET. The results also determined the values of the repetition rate and the exposure time required in order to obtain the value of the required radioactivity, where four values were obtained.

This study can be expanded in order to study the effect of the geometric dimensions of the vacuum chamber and the possibility of modifying them for increasing the radioactivity.

We expect that in the current operational conditions, the operating energy of the dense plasma focus device should not be less than 100 kJ in order to obtain the required radioactivity of ^{13}N isotope.

REFERENCES

1. **Mather J. W.,** Formation of a high-density deuterium plasma focus, Phys. Fluids. 8 (2) (1965) 366–377.
2. **Filippov N. V., Filippova T. I., Vinogradov V. P.,** Dense high-temperature plasma in a non-cylindrical Z-pinch compression, Nucl. Fusion, Suppl. Part 2 (January) (1962) 577.
3. **Haines M. G.,** A review of the dense Z-pinch, Plasma Phys. Control. Fusion. 53 (9) (2011) 093001.
4. **Al-Hawat S., Akel M., Lee S., Saw S. H.,** Model parameters versus gas pressure in two different plasma focus devices operated in argon and neon, J. Fusion Energy. 31 (1) (2012) 13–20.
5. **Lee S., Saw S. H.,** Plasma focus ion beam fluence and flux – For various gases, Phys. Plasmas. 20 (6) (2013) 062702.
6. **Mohamed A. E. S.,** A dense plasma focus device as a pulsed neutron source for material identification, A dissertation for the degree of Ph.D., Kansas State University, Kansas, USA, 2015.
7. **Feugeas J. N., Llonch E. C., De González C. O., Galambos G.,** Nitrogen implantation of AISI 304 stainless steel with a coaxial plasma gun, J. Appl. Phys. 64 (5) (1988) 2648–2651.
8. **Rawat R. S., Srivastava M. P., Tandon S., Mansingh A.,** Crystallization of an amorphous lead zirconate titanate thin film with a dense-plasma-focus device, Phys. Rev. B. 47 (9) (1993) 4858–4862.
9. **Kant C. R., Srivastava M. P., Rawat R. S.,** Thin carbon film deposition using energetic ions of a dense plasma focus, Phys. Lett. A. 226 (3–4) (1997) 212–216.
10. **Tan K. S.,** High growth rate synthesis of zinc oxide and carbon based nanostructured materials using dense plasma focus device, A dissertation for the degree Ph.D, Nanyang Technological University, Singapore, 2017.
11. **Rawat R. S.,** Dense plasma focus – High-energy-density pulsed plasma device based novel facility for controlled material processing and synthesis, In book: Plasma Science and Technology for Emerging Economies, Springer, Singapore (2017) 39–112.
12. **Zhang T., Lin J., Patran A., et al.,** Optimization of a plasma focus device as an electron beam source for thin film deposition, Plasma Sources Sci. Technol. 16 (2) (2007) 250–256.

13. **Pimenov V. N., Demina E. V., Ivanov L. I., et al.,** Damage and modification of materials produced by pulsed ion and plasma streams in Dense Plasma Focus device, Nukleonika. 53 (3) (2008) 111–121.

14. **Gribkov V. A.,** Physical processes taking place in dense plasma focus devices at the interaction of hot plasma and fast ion streams with materials under test, Plasma Phys. Control. Fusion. 57 (6) (2015) 065010.

15. **Roshan M. V., Lee P., Lee S., et al.,** Backward high energy ion beams from plasma focus, Phys. Plasmas. 16 (7) (2009) 074506.

16. **Brzosko J. S., Nardi V.,** High yield of ^{12}C (*d*, *n*) ^{13}N and ^{14}N (*d*, *n*) ^{15}O reactions in the plasma focus pinch, Phys. Lett. A. 155 (2–3) (1991) 162–168.

17. **Roshan M. V., Razaghi S., Asghari F., et al.,** Potential medical applications of the plasma focus in the radioisotope production for PET imaging, Phys. Lett. A. 378 (30–31) (2014) 2168–2170.

18. **Sumini M., Mostacci D., Rocchi F., et al.,** Preliminary design of a 150 kJ repetitive plasma focus for the production of 18-F, Nucl. Instrum. Methods Phys. Res. A. 562 (2) (2006) 1068–1071.

19. **Shirani B., Abbasi F.,** Prospects for ^{13}N production in a small plasma focus device, J. Fusion Energy. 32 (2) (2013) 235–241.

20. **Akel M., Alsheikh Salo S., Ismael S., et al.,** Interaction of the high energy deuterons with the graphite target in the plasma focus devices based on Lee model, Phys. Plasmas. 21 (7) (2014) 072507.

21. **Sadeghi H., Amrollahi R., Fazelpour S., Omrani M.,** Simulation of dense plasma focus devices to produce N-13 efficiently, Laser Part. 37 (2) (2019) 209–216.

22. **Lee S., Saw S. H.,** Plasma focus ion beam fluence and flux – Scaling with stored energy, Phys. Plasmas. 19 (11) (2012) 112703.

23. **Lee S., Saw S. H.,** The plasma focus – Numerical experiments, insights and application, In book: Plasma Science and Technology for Emerging Economies: An AAAPT Experience, Rawat R. S. (Editor), Springer, Singapore, 2017. 811 p. Pp. 131–137.

24. **Soto L.,** New trends and future perspectives on plasma focus research, Plasma Phys. Control. Fusion. 47 (5A) (2005) A361.

25. **Carlqvist P.,** Current limitation and solar flares, Sol. Phys. 7 (3) (1969) 377–392.

26. **Talaei A., Sadat Kiai S. M.,** Study the influence of the bank energy on the dynamical pinch in plasma focus, J. Fusion Energy. 28 (3) (2009) 304–313.

27. **Young F. C., Golden J., Kapetanakos C. A.,** Diagnostics for intense pulsed ion beams, Rev. Sci. Instrum. 48 (4) (1977) 432–443.

28. www.srim.org for the stopping and range of ions in matter.

29. **Michelmann R.,** https://www-nds.iaea.org/exfor/exfor.htm.

30. **Castillo S.,** Medical and statistical review of N-13 ammonia Positron Emission Tomography, 1999, Florence Houn, MD MPH FACP, Medical Office.

СПИСОК ЛИТЕРАТУРЫ

1. **Mather J. W.** Formation of a high-density deuterium plasma focus // Physics of Fluids. 1965. Vol. 8. No. 2. Pp. 366–377.

2. **Filippov N. V., Filippova T. I., Vinogradov V. P.** Dense high-temperature plasma in a non-cylindrical Z-pinch compression // Nuclear Fusion. Supplement. 1962. Part 2. January. P. 577.

3. **Haines M. G.** A review of the dense Z-pinch // Plasma Physics and Controlled Fusion. 2011. Vol. 53. No. 9. P. 093001.

4. **Al-Hawat S., Akel M., Lee S., Saw S. H.** Model parameters versus gas pressure in two different plasma focus devices operated in argon and neon // Journal of Fusion Energy. 2012. Vol. 31. No. 1. Pp. 13–20.

5. **Lee S., Saw S. H.** Plasma focus ion beam fluence and flux – For various gases // Physics of Plasmas. 2013. Vol. 20. No. 6. P. 062702.

6. **Mohamed A. E. S.** A dense plasma focus device as a pulsed neutron source for material identification. A dissertation for the degree of Ph.D. Kansas, USA: Kansas State University, 2015. 168 p.

7. **Feugeas J. N., Llonch E. C., De González C. O., Galambos G.** Nitrogen implantation of AISI 304 stainless steel with a coaxial plasma gun // Journal of Applied Physics. 1988. Vol. 64. No. 5. Pp. 2648–2651.

8. **Rawat R. S., Srivastava M. P., Tandon S., Mansingh A.** Crystallization of an amorphous lead zirconate titanate thin film with a dense-plasma-focus device // Physical Review B. 1993. Vol. 47. No. 9. Pp. 4858–4862.

9. **Kant C. R., Srivastava M. P., Rawat R. S.** Thin carbon film deposition using energetic ions of a dense plasma focus // Physics Letters A. 1997. Vol. 226. No. 3–4. Pp. 212–216.

10. **Tan K. S.** High growth rate synthesis of zinc oxide and carbon based nanostructured materials using dense plasma focus device. A dissertation for the degree of Ph.D. Singapore: Nanyang Technological University, 2017.

11. **Rawat R. S.** Dense plasma focus – high-energy-density pulsed plasma device based novel facility for controlled material processing and synthesis // Plasma Science and Technology for Emerging Economies: An AAAPT Experience. Rawat R. S. (Editor). Singapore: Springer, 2017. 811 p. Pp. 39–112.

12. **Zhang T., Lin J., Patran A., Wong D., Hassan S. M., Mahmood S., Rawat R. S.** Optimization of a plasma focus device as an electron beam source for thin film deposition // Plasma Sources Science and Technology. 2007. Vol. 16. No. 2. Pp. 250–256.

13. **Pimenov V. N., Demina E. V., Ivanov L. I., Gribkov V. A., Dubrovsky A. V., Ugaste U., Tartari A.** Damage and modification of materials produced by pulsed ion and plasma streams in Dense Plasma Focus device // Nukleonika. 2008. Vol. 53. No. 3. Pp. 111–121.

14. **Gribkov V. A.** Physical processes taking place in dense plasma focus devices at the interaction of hot plasma and fast ion streams with materials under test // Plasma Physics and Controlled Fusion. 2015. Vol. 57. No. 6. P. 065010.

15. **Roshan M. V., Lee P., Lee S., Talebitaher A., Rawat R. S., Springham S. V.** Backward high energy ion beams from plasma focus // Physics of Plasmas. 2009. Vol. 16. No. 7. P. 074506.

16. **Brzosko J. S., Nardi V.** High yield of ^{12}C (d, n)^{13}N and ^{14}N (d, n)^{15}O reactions in the plasma focus pinch // Physics Letters A. 1991. Vol. 155. No. 2–3. Pp. 162–168.

17. **Roshan M. V., Razaghi S., Asghari F., Rawat R. S., Springham S. V., Lee P., Tan T. L.** Potential medical applications of the plasma focus in the radioisotope production for PET imaging // Physics Letters A. 2014. Vol. 378. No. 30–31. Pp. 2168–2170.

18. **Sumini M., Mostacci D., Rocchi F., Frignani M., Tartari A., Angeli E., Cucchi G.** Preliminary design of a 150 kJ repetitive plasma focus for the production of 18-F // Nuclear Instruments and Methods in Physics Research. Section A: Accelerators, Spectrometers, Detectors and Associated Equipment. 2006. Vol. 562. No. 2. Pp. 1068–1071.

19. **Shirani B., Abbasi F.** Prospects for ^{13}N production in a small plasma focus device // Journal of Fusion Energy. 2013. Vol. 32. No. 2. Pp. 235–241.

20. **Akel M., Alsheikh Salo S., Ismael S., Saw S. H., Lee S.** Interaction of the high energy deuterons with the graphite target in the plasma focus devices based on Lee model // Physics of Plasmas. 2014. Vol. 21. No. 7. P. 072507.

21. **Sadeghi H., Amrollahi R., Fazelpour S., Omrani M.** Simulation of dense plasma focus devices to produce N-13 efficiently // Laser and Particle Beams. 2019. Vol. 37. No. 2. Pp. 209–216.

22. **Lee S., Saw S. H.** Plasma focus ion beam fluence and flux – Scaling with stored energy // Physics of Plasmas. 2012. Vol. 19. No. 11. P. 112703.

23. **Lee S., Saw S. H.** The plasma focus – Numerical experiments, insights and application // Plasma Science and Technology for Emerging Economies: An AAAPT Experience. Rawat R. S. (Editor). Singapore: Springer, 2017. 811 p. Pp. 131–137.

24. **Soto L.** New trends and future perspectives on plasma focus research // Plasma Physics and Controlled Fusion. 2005. Vol. 47. No. 5A. P. A361.

25. **Carlqvist P.** Current limitation and solar flares // Solar Physics. 1969. Vol. 7. No. 3. Pp. 377–392.

26. **Talaei A., Sadat Kiai S. M.** Study the influence of the bank energy on the dynamical pinch in plasma focus // Journal of Fusion Energy. 2009. Vol. 28. No. 3. Pp. 304–313.

27. **Young F. C., Golden J., Kapetanakos C. A.** Diagnostics for intense pulsed ion beams // Review of Scientific Instruments. 1977. Vol. 48. No. 4. Pp. 432–443.

28. www.srim.org for the stopping and range of ions in matter

29. **Michelmann R.** https://www-nds.iaea.org/exfor/exfor.htm

30. **Castillo S.** Medical and Statistical Review of N-13 Ammonia Positron Emission Tomography. 1999. Florence Houn, MD MPH FACP, Medical Office.

THE AUTHORS

NASSIF Alaa
Al-Wataniya Private University
Al-Wataniya Private University, International Hama–Homs Highway, Hama, XQ92+PMC, Syrian Arab Republic
alaa.nassif.85@hotmail.com

SAHYOUNI Walid
Al-Baath University
Al-Baath University, Damascus – Aleppo Highway, Homs, PP75+5VC, Syrian Arab Republic
wsahyouni@albaath-univ.edu.sy

ZEIDAN Ola
Al-Baath University
Al-Baath University, Damascus – Aleppo Highway, Homs, PP75+5VC, Syrian Arab Republic
ozedan@albaath-univ.edu.sy

KAFA Noha
Al-Baath University
Al-Baath University, Damascus – Aleppo Highway, Homs, PP75+5VC, Syrian Arab Republic
nohakafa10@gmail.com

СВЕДЕНИЯ ОБ АВТОРАХ

НАССИФ Алаа – *доктор военных наук, профессор инженерного факультета Частного университета Аль-Ватания, г. Хама, Сирийская Арабская Республика.*
XQ92+PMC, Syrian Arab Republic, Hama, Al-Wataniya Private University
alaa.nassif.85@hotmail.com

САХЬЮНИ Валид – *Ph.D., профессор кафедры физики (исследовательский отдел физики плазмы) Университета Аль-Баас, г. Хомс, Сирийская Арабская Республика.*
PP75+5VC, Syrian Arab Republic, Homs, Damascus – Aleppo Highway
wsahyouni@albaath-univ.edu.sy

ЗЕЙДАН Ола – *Ph.D., профессор кафедры физики (исследовательский отдел физики плазмы) Университета Аль-Баас, г. Хомс, Сирийская Арабская Республика.*
PP75+5VC, Syrian Arab Republic, Homs, Damascus – Aleppo Highway
ozedan@albaath-univ.edu.sy

КАФА Ноха – *сотрудник кафедры физики Университета Аль-Баас, г. Хомс, Сирийская Арабская Республика.*
PP75+5VC, Syrian Arab Republic, Homs, Damascus – Aleppo Highway
nohakafa10@gmail.com

Received 25.02.2023. Approved after reviewing 20.03.2023. Accepted 20.03.2023.
Статья поступила в редакцию 25.02.2023. Одобрена после рецензирования 20.03.2023. Принята 20.03.2023.